

Magnetic breakdown in cadmium

V. A. Ventsel', O. A. Voronov, and A. V. Rudnev

Institute of High-Pressure Physics

(Submitted December 17, 1977)

Zh. Eksp. Teor. Fiz. 73, 246-256 (July 1977)

The effective masses and the Dingle factor for all the oscillations in the $(10\bar{1}0)$ and $(11\bar{2}0)$ planes were determined by measuring, in pulsed magnetic fields up to 150 kOe, the dependence of the oscillation amplitudes in the de Haas-van Alphen effect on the temperature and on the magnetic field. An anomalous angular dependence of the Dingle factor was observed for the Dingle factor at the frequency $F_{\gamma/3}$ and is attributed to magnetic breakdown. The areas and positions in k -space of the extremal magnetic-breakdown orbits, the parameters v_1 and v_2 at the breakdown points, the gap Δ between the first and second Brillouin zone at the breakdown points are all calculated. The experimental data are used to estimate the gap Δ . A possible interpretation, based on magnetic breakdown, is offered for the oscillation frequency f_x .

PACS numbers: 75.20.En, 75.30.Cr, 71.25.Jd

The Fermi surface (FS) of cadmium was investigated in detail experimentally with the aid of galvanomagnetic phenomena,^[1] the de Haas-van Alphen effect,^[2-4] the size effect,^[7] and cyclotron resonance.^[8-10] As a result of these measurements, it is presently regarded as established that the hole part of the FS consists of pockets in the first Brillouin zone (BZ) and a monster in the second BZ. The horizontal arms of the monster are torn and it can be represented in the form of undulating figures that are elongated along the HK edges and have, in the section with the ΓKM plane, the appearance of three foils that are joined together near the edge at the point K . The electron surfaces in the third BZ take the form of a lens located at the center of the Γ zone. In the model of almost-free electrons^[11] cadmium should have also FS parts in the form of a butterfly in the third BZ and a cigar in the fourth BZ, but the existence of these sections has not yet been experimentally confirmed.

The intersection of the monster with the ΓKM plane, which takes the form of a trefoil, has been dubbed the γ section, and Tsui and Stark^[2] have shown that as a result of magnetic breakdown this section can be realized both in the form of a complete γ section, and in the form of orbits that pass only along one of the foils ($\frac{1}{3}\gamma$) or along two foils ($\frac{2}{3}\gamma$). Measurements of this kind were made only in a narrow angle interval near the $H \parallel [0001]$ direction, and the data obtained by measuring the cyclotron resonance^[8-10] were the results of measurements made in fields too weak to yield the values of the effective masses $m_{\gamma/3}$ and $m_{2\gamma/3}$.

We report here measurements of the oscillation amplitudes in the de Haas-van Alphen effect, particularly the amplitudes of the oscillations connected with the sections γ , $\frac{2}{3}\gamma$, and $\frac{1}{3}\gamma$, for the purpose of ascertaining the character of the phenomena connected with magnetic breakdown on these sections, and to determine the effective masses of the electrons that move along these orbits.

The amplitude of the oscillations connected with the k -th extremal cross section, has in the de Haas-van Alphen effect the following dependence on the temperature and on the magnetic field:

$$A_k(H, T) = A_{0k} H^\alpha T \exp\left(-\frac{2\pi^2 m^* c k (T+x)}{e\hbar H}\right), \quad (1)$$

where m^* is the effective mass of the electron, x is the Dingle temperature, and the exponent α depends on the experimental procedure and is equal, in particular, to $-\frac{1}{2}$ in measurements by a resonance method in pulsed magnetic fields. From the temperature dependence of the oscillation amplitude it is possible to calculate the effective mass m^* , and from the dependence of the amplitude on the magnetic field we can determine the Dingle temperature. The Dingle temperature is governed by the average electron relaxation time on the given orbit, and has been shown^[14] to depend little on the magnetic-field direction.

If a given orbit is the result of magnetic breakdown, then the oscillation amplitude $A_k(H, T)$ is determined not only by expression (1), but also by the factor $P_k(H)$, which is proportional to the probability of the existence of an extremal section with a given area S_k :

$$\bar{A}_k(H, T) = A_k(H, T) P_k(H). \quad (2)$$

The exact solution of the problem of electron-motion under the conditions of magnetic breakdown on one Bragg reflection plane was obtained by Slutskin and Kadigrobov.^[15] Within the framework of the same assumptions, Kochkin^[16] has calculated rigorously the amplitudes of the oscillations in the de Haas-van Alphen effect for the particular case of two bands separated by one Bragg-reflection plane.

In cadmium breakdown on orbits of type γ is realized near the edge HK of the band, where three Bragg-reflection planes intersect. If the distance between the breakdown planes is large, i.e., the breakdown acts on each of the planes can be treated independently, then, as shown by Kochkin,^[16] it is possible to use the quasiclassical approximation to calculate, at least for the fundamental harmonic, the probability of the passage of an electron along a given orbit, using the expression

$$P(H) = \sum_i \prod_{i,j} p_i^{1/2} q_j^{1/2}, \quad (3)$$

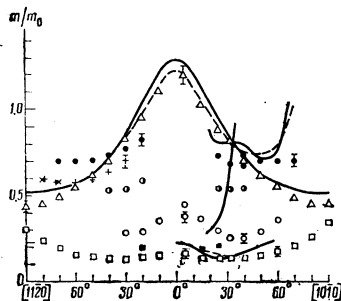


FIG. 1. Effective masses m/m_0 in cadmium in relative units: \square —section of pocket α , \blacksquare —monster section β , \circ —monster section $\frac{1}{3}\gamma$. (The lower point at $\varphi=5^\circ$ in the $(11\bar{2}0)$ plane pertains to the lower branch $S_{1/3\gamma}$ in the frequency spectrum.^[6]) \bullet —monster section $\frac{2}{3}\gamma$, \bullet —monster section γ (at $\varphi=40^\circ$ in the $(11\bar{2}0)$ plane, the lower point pertains to the γ_2^2 branch and the upper to the γ_2^1 branch^[6]), \triangle —lens section λ , $+$ —monster section σ , \times —monster section A . The solid line is drawn through the data of^[9] and the dashed one through the data of^[10].

where p_i is the breakdown probability at the i -th point of the BZ, and $q_j = 1 - p_j$ is the probability of reflection at the j -th point. The summation is over all possible trajectories l of the given type, and the numbers of the breakdown points i and reflection points j are chosen such as to realize a trajectory of the given type. The probability p_i takes the form $\exp(-H_{0i}/H)$, where H_{0i} is the breakdown field in the i -th point of the BZ this field is expressed in terms of the spectrum parameters as follows:

$$H_{0i} = \frac{\pi c}{4\hbar e} \frac{\Delta_i^2}{|v_{\parallel}^{(i)} v_{\perp}^{(i)}|}, \quad (4)$$

where the energy gap Δ_i is taken at the i -th breakdown point, while $v_{\parallel}^{(i)}$ and $v_{\perp}^{(i)}$ are the tangential and normal projections, on the Bragg reflection plane, of the free-electron velocity component perpendicular to the direction of the magnetic field.

Thus, if the existence of a given extremal FS section is connected with the magnetic-breakdown phenomenon, then the Dingle factor in expression (1) for the oscillation amplitude should be replaced by the factor

$$\exp(-2\pi^2 m^* c k x / e \hbar H) P(H).$$

When the Dingle temperature is determined from the slope of $\ln(AH^{-\alpha})$ as a function of $1/H$ in a limited magnetic-field interval, the quantity actually determined is the virtual temperature x^* . The quantity x^* determined in this manner can be larger than x if $P(H)$ is determined mainly by terms of the type $\exp(-H_0/H)$, and smaller than x if $P(H)$ decreases with increasing field like $(1 - \exp(-H_0/H))$. Assuming that the temperature x is approximately the same for all FS sections and does not depend on the direction of the magnetic field,^[14] we can separate from x^* the part connected with the magnetic breakdown and, using expressions (3) and (4), calculate the energy gap Δ and then compare it with the value determined from theoretical calculations, say in the pseudopotential approximation.

EXPERIMENTAL PROCEDURE

The de Haas-van Alphen effect was measured in a pulsed magnetic field whose maximum value reached 150 kOe. The setup and the method used to measure the oscillations are similar to those described in^[11,18]. In the planes (1010) and $(11\bar{2}0)$, in steps of 10° , samples measuring $1 \times 1 \times 5$ mm were cut from a bulky single crystal, with a specified direction of the crystallographic axes relative to the longitudinal axis of the sample; this orientation was refined each time by x-ray diffraction, accurate to 1° . The resistance ratio $R_{300\text{ K}}/R_{4.2\text{ K}}$ was $\gtrsim 15000$ for the samples from this batch.

The temperature dependence of the oscillation amplitude was measured as helium vapor was pumped on in the temperature range from 4.2 to 1.6 K. At the lowest temperature we measured the dependence of the oscillation amplitude on the magnetic field. For subsequent computer reduction of the results, the picture of the oscillations was photographed at 21 values of the capacitor voltages from 1000 to 3000 V. We then measured the amplitude of the resonance bursts for increasing and decreasing fields. We thus obtained 42 points on the $A(H)$ plot.

MEASUREMENT RESULTS

a) *Determination of the electron effective masses.* The effective masses m^* were determined graphically from the slope of $\ln(A/T)$ as a function of T for all the observed oscillation frequencies. The results of these measurements are shown in Fig. 1. The effective mass for the sections of the pocket α , equal to $0.16m_0$ at $H \parallel [0001]$, decreases to $0.13m_0$ when the field is deflected away from this direction in the (1010) and $(11\bar{2}0)$ planes through an angle $\sim 30^\circ$, and then increases to $m/m_0 = 0.3$ at $H \parallel [11\bar{2}0]$ and 0.33 at $H \parallel [10\bar{1}0]$.

For the section β , reliable data were obtained only at a field deflection $15\text{--}20^\circ$ from the $[0001]$ axis. The masses connected with the monster section γ were measured in the angle interval $20^\circ < \varphi < 70^\circ$ in both crystallographic planes, i.e., where the oscillation amplitude is large enough. In the $(11\bar{2}0)$ plane the mass m_γ depends little on the orientation and amounts to $0.7m_0$, while in the (1010) plane the dependence on the angle is stronger — m_γ decreases from a value $0.83m_0$ at $\varphi = 20^\circ$ to a value $0.7m_0$ at $\varphi = 70^\circ$. The electron masses for the $\frac{2}{3}\gamma$ section were measured in a narrow angle interval $20^\circ < \varphi < 40^\circ$ and are close in magnitude to $m/m_0 = 0.5$. In the $(11\bar{2}0)$ plane we have $m_{2/3\gamma}/m_\gamma = \frac{2}{3}$ accurate to $\sim 12\%$, and in the (1010) plane this ratio holds true accurate to 3% at $\varphi = 20^\circ$ at 6% at $\varphi = 40^\circ$, i.e., worse the closer $m_{2/3\gamma}$ is to $0.5m_0$. The effective mass of the section $\frac{1}{3}\gamma$ was measured in the angle interval $\varphi < 30^\circ$ in the (1010) plane and $\varphi < 60^\circ$ in the $(11\bar{2}0)$ plane. In the (1010) plane the mass decreases from $0.35m_0$ at $\varphi = 10^\circ$ to $0.29m_0$ at $\varphi = 30^\circ$, which agrees within 10–15% with the ratio $m_{1/3\gamma}/m_\gamma = \frac{1}{3}$. In the $(11\bar{2}0)$ plane $m_{1/3\gamma}$ decreases from $\sim 0.45m_0$ at $\varphi = 5^\circ$ to $m = 0.25m_0$ at $30\text{--}40^\circ$, and then increases to $m = 0.36m_0$ at $\varphi = 60^\circ$. Near the minimum the value of $m_{1/3\gamma}$ is one-third the value of m_γ within 10%, and when φ is increased to 60°

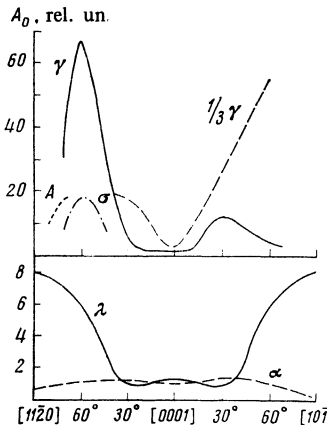


FIG. 2. Amplitudes of oscillations A_0 in relative units for different sections of the Fermi surface that do not depend on the value of the magnetic field H .

the difference between $m_{\gamma/3}$ and $(\frac{1}{3})m_\gamma$, reaches 40%.

The effective mass connected with the lens section was measured in the entire angle range and ranges from $1.2m_0$ at $\varphi \sim 0^\circ$ to $0.44m_0$ at $H \perp [0001]$. The oscillations with frequencies designated A and σ in^[5] were observed in the angle intervals $70^\circ < \varphi < 80^\circ$ and $30^\circ < \varphi < 80^\circ$ respectively in the $(10\bar{1}0)$ plane. $m_A \sim 0.6m_0$, while m_σ decreases smoothly from $\sim 0.7m_0$ at 30° to $0.6m_0$ at $\varphi = 80^\circ$.

The lines in Fig. 1 show the values of m/m_0 obtained by the cyclotron-resonance method.^[8-10] It is seen that the masses obtained from the temperature dependences of the oscillation amplitudes are smaller than the masses obtained by the cyclotron-resonance method. The difference is $\sim 10\%$ for the pocket α , $\sim 25\%$ for the monster section β , $\sim 7\%$ for the section γ , and $\sim 10\%$ for the lens at $H \perp [0001]$.

Since the referred-to FS sections of cadmium are quite simple, the effective masses should be external at the same values of k_z at which the areas of the FS sections are extremals, i.e., the effective masses measured in both methods are connected with the same orbits. It appears that one of the causes of the discrepancy may be the dependence of the electron-phonon renormalization $m^* = m(1 + \lambda)$ of the effective mass on the field and on the temperature,^[19] obtained on the basis of^[20]. The field dependence of λ has not been considered in the literature in the case of cadmium, but it has been shown^[19] that for the β section in mercury, in the temperature interval 2.2–4.2 K and in fields 50–300 kOe, the change in mass reaches 34%. The effective value of λ decreases with increasing field, and therefore the masses obtained by measuring the amplitudes of the oscillations in fields ~ 100 kOe should be less than the masses obtained in fields ~ 100 Oe by the cyclotron-resonance method. It would be apparently of interest in this connection to determine the $m^*(H)$ dependence directly.

The data for other sections cannot be compared, since they were either measured at other orientations of the magnetic field, or were not observed at all (in one of the studies). It should be noted that although the cyclotron-resonance method is much more accurate than measurements of the temperature dependence of the oscillation amplitude, the interpretation of the latter is much sim-

pler, since the masses determined by this method are directly connected with definite sections of the FS, whereas the identification of the masses measured by the cyclotron-resonance method with definite sections of the Fermi surface is a more complicated procedure. It appears therefore that the most reliable interpretation can be obtained by comparing the cyclotron-resonance data with those on the de Haas–van Alphen effect.

b) *Determination of the Dingle factor.* The Dingle factor was calculated for all the FS sections in the angle interval where the oscillation amplitudes were high enough. To calculate the value of x we used those values of the effective masses which were obtained from the temperature dependences of the oscillation amplitudes, since these mass values were obtained for the same samples and in the same magnetic-field interval, thus automatically ensuring the correct value of the coefficient in the exponential when the Dingle temperature was determined.

For all the FS sections, except γ and $\frac{1}{3}\gamma$, the Dingle temperature is ~ 1 K. For the γ section, the apparent Dingle temperature is $x^* \sim 0.5$ K, and for the $\frac{1}{3}\gamma$ section the temperature x^* obtained in the manner described above is strongly dependent on the orientation. The apparent Dingle temperature increases from ~ 1 K at $\varphi \sim 0^\circ$ when the field is inclined away from the hexagonal axis, and reaches $x^* \sim 4$ K at $\psi = 20^\circ$ in the $(10\bar{1}0)$ plane and $x^* \sim 6$ K at $\varphi = 60^\circ$ in the $(11\bar{2}0)$ plane.

Figure 2 shows the amplitude A_0 , which does not depend on the magnetic field, for all the observed oscillations, as well as the angle intervals in which the various oscillations are observed. The values of A_0 were obtained by dividing the measured amplitudes by the quantity

$$H^{-\frac{1}{2}} \exp\left(-\frac{2\pi^2 m c k (T+x)}{e \hbar H}\right)$$

The curves are broken in those places where the Dingle factor could not be determined by experiment.

DISCUSSION OF RESULTS

1. The abrupt increase of the Dingle factor for the oscillations connected with the $\frac{1}{3}\gamma$ section when the magnetic field is deflected away from the $[0001]$ axis can be associated with magnetic breakdown. Figure 3 shows the intersection of the monster and of the pocket with the $ATKH$ plane, and a number of intersections of this figure with planes parallel to the basal plane. Section a corresponds to the extremal section of the pocket, b corresponds to an intermediate section that can become, as will be shown below, extremal as a result of magnetic breakdown, c corresponds to the central γ section, and d is realized at a certain distance from the basal plane and corresponds to monster section in which a pocket section is imbedded. The monster section γ arises only when the trefoil is followed over the entire surface of all three foils, a fact that corresponds to absence of breakdown (orbit 1234567891 on Fig. 3d), or to complete breakdown of all the gaps (motion along the orbit 1256782345891). In the case when the breakdown

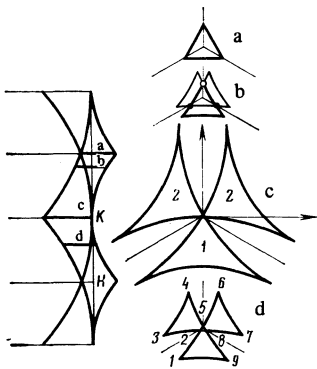


FIG. 3. Intersection of the monster with the ATKH plane and with planes (a, b, c, d) perpendicular to the [0001] axis.

does not occur on all the plane, the orbits realized are either $\frac{2}{3}\gamma$ (trajectory of the type 12567891 with breakdown at the points 2 and 5 and with reflection at the point 8), or else $\frac{1}{3}\gamma$ (trajectory of the type 125891 with breakdown at the points 2 and 8 and reflection at the point 5).

The breakdown field H_{0i} was calculated by a least-squares method in which the experimentally determined $A(H)$ dependence was compared with expression (2). When the field is inclined to the hexagonal axis, the breakdown fields at the points 2, 5, and 8 can become unequal; the calculation was therefore carried out for three different fields H_{0i} . The factor $P(H)$ for the $\frac{1}{3}\gamma$ section took the form

$$P_{\gamma/3}(H) = \exp\left(-\frac{H_{01}}{2H}\right) \exp\left(-\frac{H_{02}}{2H}\right) \left[1 - \exp\left(-\frac{H_{03}}{H}\right)\right]^{\frac{1}{2}}. \quad (5)$$

The form for the γ section was

$$P_\gamma(H) = \prod_{i=1}^3 \left[1 - \exp\left(-\frac{H_{0i}}{H}\right)\right]^{\frac{1}{2}} + \prod_{i=1}^3 \exp\left(-\frac{H_{0i}}{H}\right). \quad (6)$$

The best agreement between the experimentally observed $A(H)$ dependence and expressions (2), (5), and (6) was reached by adjusting the values of H_{01} , H_{02} , and H_{03} . It was assumed here, as for all other sections, that the Dingle factor is $x \approx 1$ K.

For the $\frac{1}{3}\gamma$ section at large values of the breakdown field, the value of $P_{\gamma/3}(H)$ depends little on the choice of H_{03} and is determined mainly by the value of $H_0 = \frac{1}{2} \times (H_{01} + H_{02})$. Figure 3 shows a plot of H_0 obtained in this manner for various orientations; the possible error in the determination of H_0 , due to the inaccuracy of the calculation of m^* and to the scatter in the experimental dependence, is shown shaded in the figure. Calculations for the γ section have shown that in the field interval 30–100 kOe used in the experiment $P_\gamma(H)$ depends little on the field and decreases with increasing H . This leads to a decrease of the apparent Dingle temperature, and accounts in fact for the values $x^* \sim 0.5$ K, which are lower than for the other sections (~ 1 K).

The oscillations connected with the $\frac{1}{3}\gamma$ section are observed in a pulsed magnetic field when H is inclined to the [0001] axis up to 60° in the (1120) plane and only near $H \parallel [0001]$ when the modulation procedure is used.^[5] Since H_0 increases abruptly when H is deflected from

the [0001] axis, observation of the frequencies $F_{\gamma/3}$ calls for strong fields, which are attainable by the pulse method. On the other hand, in strong field the argument $2\pi h/fH^2$ of the Bessel function becomes small (h is the amplitude of the modulating field), and consequently the Bessel function itself, which determines the amplitude $\varepsilon_n \sim J_n(2\pi hF/H^2)A_{1/3,\gamma}(H)$ of the signal in the receiving coil in measurements at the n -th harmonic of the modulation field, also becomes small. Therefore the product $J_n A_{1/3,\gamma}(H)$ may turn out to be small in the entire field interval, and this explains the narrowness of the region where the frequency $F_{\gamma/3}$ is observed near $H \parallel [0001]$ in constant fields.^[5]

2. To explain the obtained $H_0(\varphi)$ dependence it is necessary to determine the coordinates of the breakdown points and to calculate at these points the value of $|v_{\parallel}v_{\perp}|$, which enters in expression (4). This calls for determining those values of k_z at which the Sections $S_{\gamma/3}$ are extremal, and it is necessary to construct for these k_z the trajectories corresponding to the motion of the free electrons. The intersection of the latter trajectories with the Bragg-reflection planes yields the coordinates of the breakdown points. The determination of the extremal sections $S_{\gamma/3}$ in the many-wave approximation calls for a large volume of computer calculations, and the qualitative picture was obtained by carrying out the entire calculation in the single-wave approximation. In order that the horizontal arms of the monster be broken, we introduced an additional assumption, namely, the parameter b of the Brillouin zone was decreased by 15%.

It is seen from Fig. 3c that the foils 1 and 2 are not equivalent with respect rotation about the axes [1010] and [1120]. We therefore calculated the extremal sections for four cases of rotation of the foils 1 and 2 about the axes [1010] and [1120] in steps of 10° . Figure 5 shows the results of these calculations for the angles $\varphi = 0^\circ$, 30° , and 60° . The filled symbols in the figures denote the breakdown points, and the light ones the reflection points, which are needed for the existence of the magnetic-breakdown section $\frac{1}{3}\gamma$.

The calculation yielded the following quantities:

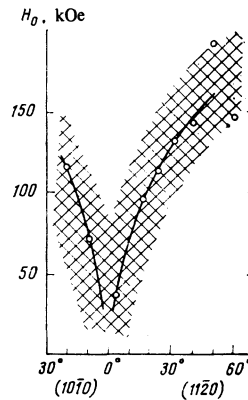


FIG. 4. Calculated values of the breakdown field H_0 for the section $\frac{1}{3}\gamma$ of the monster. The shaded area is the region of the possible scatter due to the experimental errors in the determination of the effective masses and of the field dependence of the amplitude.

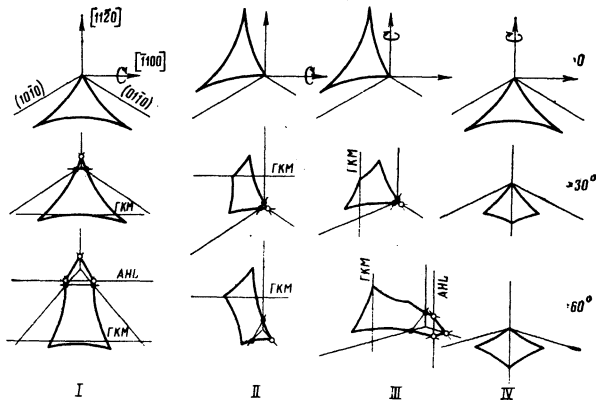


FIG. 5. Calculated extremal sections $S_{1/3}$ for different orientations of the magnetic field relative to the crystallographic axes, $= 0^\circ, 30^\circ$, and 60° respectively.

a) The angular dependence of the extremal sections $S_{1/3}$ for the foils 1 and 2. The upper part of Fig. 6 shows, in relative units, the calculation results and the experimental data. It is seen that orbits II and IV on Fig. 4 duplicate qualitatively the course of the experimental curves. The lower group of the experimental points in the $\frac{1}{3}\gamma$ series on Fig. 6 can pertain either to branches I and III, or to a superposition of the frequencies $(F_\beta + F_{\gamma/3})/2$.

b) The coordinates of the breakdown points and the components $v_{||}$ and v_{\perp} of the free-electron velocity for these points.

c) The energy gap Δ between the first and second Brillouin zones calculated along the lines passing through the breakdown points on planes of the type $HKLM$, in the approximation of nine plane wave without allowance for the spin-orbit interaction. The form factors of the pseudopotentials were taken from^[6], where they were obtained from the experimental data with allowance for the dimensions of all the parts of the FS. Figure 7 shows the dependence of the gap Δ on the distance s_0 along the line that serves as the geometric locus of the breakdown points, from the point K to the intersection of this line with the HLA plane. This line is the trace of the intersection of the $HKLM$ plane with the free-electron sphere.

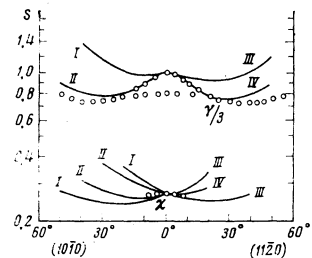


FIG. 6. Calculated angular dependence of the area of the extremal sections $\frac{1}{3}\gamma$ and χ (solid lines) and the experimental points, in relative units (it is assumed that the experimental and calculated $S_{1/3}$ are equal at $H \parallel [0001]$). The roman numerals denote the $\frac{1}{3}\gamma$ foils in the plane of rotation, as in Fig. 5.

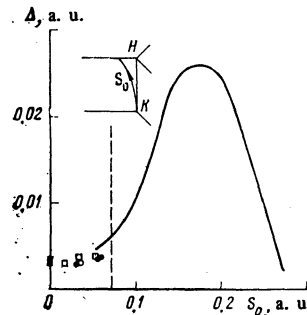


FIG. 7. Calculated dependence of the energy gap Δ between the first and second Brillouin zones along the line s_0 that passes through the breakdown points. The geometric locus of the breakdown points on one of the planes of the $HKLM$ type is shown in the upper left corner of the figure. The gap Δ was calculated from formula (4) and its symbols correspond to the cases I(○), II(□), III(●) and IV(■) shown in Fig. 5. The dashed line separates the region where the distance between the breakdown points is less than 0.01.

d) The values of $S^2 |d^2 S/dk_z^2|^{-1/2}$, calculated from the $S(k_z)$ dependence, for all four sets of the extremal values of the $\frac{1}{3}\gamma$ section. These quantities were compared with the quantities $S^2 |d^2 S/dk_z^2|^{-1/2}$ that enter in the oscillation amplitude A_0 in expression (1). It was observed that in the case of orbits II and IV the agreement with experiment is satisfactory.

Using the calculation results, we can examine the singularities in the behavior of the trajectories along foils 1 and 2 when the magnetic field is rotated in the planes (1010) and $(11\bar{2}0)$. Knowing the coordinates of the breakdown points and the value of $|v_{||}v_{\perp}|$ at these points, we can calculate H_0 from formula (4), by substituting in it the value of Δ shown in Fig. 7 (solid line), and then compare the obtained values with H_0 determined from the experimental data. Since the oscillation frequency $F_{\gamma/3}$ was observed in fields $\leq 70-80$ kOe, the values of the breakdown field $H_0 > 200$ kOe correspond to a very low breakdown probability $p \sim e^{-3}$, and it can be assumed that for $H_0 > 200$ kOe the oscillations corresponding to the given trajectory should not be observed. The value of H_0 was determined from the expression

$$H_0 = 1.84 \cdot 10^9 \frac{1}{2} \left(\frac{\Delta_1^2}{|v_{||}v_{\perp}|_1} + \frac{\Delta_2^2}{|v_{||}v_{\perp}|_2} \right), \quad (7)$$

where H_0 is in Oersteds and Δ , $v_{||}$, and v_{\perp} is in atomic units.

For all orbits shown in Fig. 5, the breakdown field calculated in this manner increases from $H_0 \sim 70$ kOe at $H \parallel [0001]$ with increasing angle φ between the direction of the magnetic field and the $[0001]$ axis. For orbits I (Fig. 5), H_0 reaches values ~ 200 kOe at $\varphi > 10^\circ$, for orbits II at $\varphi > 30^\circ$, for orbits III at $\varphi > 20^\circ$, and for orbits IV at $\varphi > 60^\circ$. It follows from the experimental data (Fig. 2) that in the $(10\bar{1}0)$ plane the branch of the spectrum with frequency $F_{\gamma/3}$ is observed at angles $\varphi < 30^\circ$, and in plane $(11\bar{2}0)$ it is observed at $\varphi < 60^\circ$. Thus, it can be concluded that the calculated $\Delta(s_0)$ dependence (Fig. 7) agrees qualitatively with experiment and that the observed oscillations with frequency $F_{\gamma/3}$

are connected with trajectories II in the (1010) plane and IV in the (1120) plane (Fig. 5). The quantities H_0 calculated for these trajectories fall, within the limits of error, in the region shown shaded in Fig. 4.

Using the values of H_0 obtained from the experimental data we can calculate the values of the gap Δ . The results of these calculations are shown in Fig. 7 in the form of points pertaining to the orbits observed in the experiment. In the region of small angles, for orbits I-III and for all angles for orbit IV the gap calculated in this manner amounts to $(3 \pm 0.6) \times 10^{-3}$ a.u. The error is connected with the inaccuracy of the calculation of H_0 (Fig. 4) from the experimental data and with the inaccuracy of the calculation of $|v_i v_k|$ as a result of the variation of the parameter b of the Brillouin zone.

We can thus estimate the gap Δ as being close to 0.003 a.u., which agrees in order of magnitude with the values of the matrix element W_{1010} cited in other papers.^[6, 21-23] This agreement should be regarded as only qualitative, since the results of our paper were obtained for breakdown points that are located at short distances from the edge of the BZ. The criterion for the suitability of formula (3) is the condition that the electron follow a quasiclassical trajectory between the breakdown acts; in other words, the area of the section of the pocket in the magnetic-breakdown section $\frac{1}{3} \gamma$ should contain more than one Landau level. If the distance between the breakdown points is α , then the area of the pocket section is $\sim \alpha^2$, and the condition $c\alpha^2/eH \gtrsim 1$ must be satisfied. In the range of magnetic fields used in the experiment, the characteristic distance α should be larger than or of the order of 0.01 a.u. in order for the quasiclassical expression (3) to be valid. This region is bounded on Fig. 7 by a dashed line. At small angles φ , for cases I, II, and III on Fig. 5 and at all angles for case IV we have $\alpha < 0.01$ a.u., and formulas (3) and (4), generally speaking, are not applicable. To obtain the dependence of the breakdown probability in this case it is necessary to solve the quantum mechanical problem of the motion of the electron under conditions of magnetic breakdown near a BZ edge and to match the solutions on these planes. To our knowledge, this problem has not been solved as yet. Nonetheless, the $P(H)$ dependence should apparently be of the form $P(H) \sim \exp(-H_0/H)$, but H_0 should no longer be determined by expression (4), although an angular dependence of the $|v_i v_k|$ type should more readily be preserved. The calculated value of Δ should therefore be regarded as being of the correct order of magnitude, and the exact value of the gap can be obtained by rigorously solving the problem.

3. The spectrum of the oscillation frequencies of cadmium includes the frequency $F_x = 5.4 \times 10^6$ Oe,^[4, 6, 24] which is observed in a narrow angle interval, $\sim 10^\circ$, near $\mathbf{H} \parallel [0001]$, but there is no reliable interpretation of this frequency. Thus, for example, according to the data of^[24], this branch can pertain both to the cigar and to the magnetic-breakdown orbit on the monster. In the calculation of the extremal cross sections of the monster, which occur in the case of magnetic breakdown through the section of the pocket, an experimental cross section

was observed close to the extremal section f the pocket α and located 0.05 a.u. away from it. This section is shown in Fig. 3b. The energy gap between the first and second zones for this section is small (large values of s_0 on Fig. 7), i.e., the parameter H_0 is small and the section should be observed in the experiment. When \mathbf{H} is inclined to the [0001] axis, the orbit begins to cross the HLA plane of the Bragg reflection and the probability of the passage of the electron along this orbit decreases. In Fig. 6, the lower group of curves corresponds to the calculated areas of this section, and the points correspond to the area of the experimentally observed extremal section. The data obtained in^[24] on the pressure dependence of S_x offer evidence in favor of the magnetic-breakdown interpretation of the section S_x .

The authors are deeply grateful to L. F. Vereshchagin for constant interest in the work, to A. I. Likhter for interest in the work and valuable discussions, and to A. A. Slutskin, V. P. Naberezhnykh, R. G. Arkhipov, and A. P. Kochkin for useful discussions.

- ¹N. E. Alekseevskii and Yu. P. Gaidukov, Zh. Eksp. Teor. Fiz. **43**, 2094 (1963) [Sov. Phys. JETP **16**, 1481 (1963)].
- ²D. C. Tsui and R. W. Stark, Phys. Rev. Lett. **16**, 19 (1966).
- ³A. S. Joseph, W. L. Gordon, J. R. Reitz, and T. G. Eck, Phys. Rev. Lett. **7**, 334 (1961).
- ⁴A. D. C. Grassie, Philos. Mag. **9**, 847 (1964).
- ⁵D. C. Tsui and R. W. Stark, The de Haas-van Alphen Spectrum of Cadmium, Preprint.
- ⁶V. A. Venttsel', O. A. Voronov, A. I. Likhter, and A. V. Rudnev, Zh. Eksp. Teor. Fiz. **70**, 272 (1976) [Sov. Phys. JETP **43**, 141 (1976)].
- ⁷R. C. Jones, R. G. Goodrich, and L. M. Falicov, Phys. Rev. **174**, 672 (1968).
- ⁸V. P. Naberezhnykh, A. A. Mar'yakhin, and V. L. Mel'nik, Zh. Eksp. Teor. Fiz. **52**, 617 (1967) [Sov. Phys. JETP **25**, 403 (1967)].
- ⁹V. P. Naberezhnykh, Doctor's Dissertation, Khar'kov, 1970.
- ¹⁰M. P. Shaw, T. G. Eck, and D. A. Zych, Phys. Rev. **142**, 406 (1966).
- ¹¹W. A. Harrison, Phys. Rev. **118**, 1190 (1960).
- ¹²I. M. Lifshitz and A. M. Kosevich, Zh. Eksp. Teor. Fiz. **29**, 730 (1955) [Sov. Phys. JETP **2**, 636 (1956)].
- ¹³R. B. Dingle, Proc. R. Soc. London Ser. A **211**, 517 (1952).
- ¹⁴D. H. Lowdes, K. M. Miller, R. G. Poulsen, and M. Springford, Proc. R. Soc. London Ser. A **331**, 497 (1973).
- ¹⁵A. A. Slutskin and A. M. Kadigrobov, Fiz. Tverd. Tela (Leningrad) **9**, 184 (1967) [Sov. Phys. Solid State **9**, 138 (1967)].
- ¹⁶A. P. Kochkin, Zh. Eksp. Teor. Fiz. **54**, 603 (1968) [Sov. Phys. JETP **27**, 324 (1968)].
- ¹⁷V. A. Venttsel', A. I. Likhter, and A. V. Rudnev, Zh. Eksp. Teor. Fiz. **53**, 108 (1967) [Sov. Phys. JETP **26**, 73 (1968)].
- ¹⁸V. A. Venttsel', Zh. Eksp. Teor. Fiz. **55**, 1191 (1968). [Sov. Phys. JETP **28**, 622 (1969)].
- ¹⁹F. M. Mueller and H. W. Myron, Commun. Phys. **1**, 99 (1976).
- ²⁰S. Engelsberg and G. Simpson, Phys. Rev. B **2**, 1657 (1970).
- ²¹S. J. Katsuki and M. Tsuji, Phys. Soc. Jpn. **20**, 1136 (1965).
- ²²A. A. Mar'yakhin and I. V. Svechkarev, Phys. Status Solidi **23**, K133 (1967).
- ²³A. A. Mar'yakhin and I. V. Svechkarev, Phys. Status Solidi **33**, K37 (1969).
- ²⁴E. S. Itskevich, A. M. Sobko, V. A. Sukhoparov, and I. M. Templeton, Paper at Fifth Intern. Conf. on Physics and Technology of High Pressures, Moscow, 1975.

Translated by J. G. Adashko